A newly designed analytical line to examine fluid inclusion isotopic compositions in a variety of carbonate samples

Emilie P. Dassié[1,2,3], Dominique Genty[3], Aurélie Noret[2], Xavier Mangenot[4,5], Marc Massault[2], Nicolas Lebas[1], Maxence Duhamel[2], Magali Bonifacie[5], Marta Gasparrini[4], Benedicte Minster[3], and Jean-Luc Michelot[2].

[1] Laboratoire d'Océanographie et du Climat: LOCEAN - IPSL, UMR 7159 CNRS/UPMC/IRD, Université P. et M. Curie, 4 place Jussieu, 75252 Paris cedex 05, France
[2] Université Paris-Sud, UMR-CNRS 8148, Geosciences Paris-Sud, Bat. 504, 91405 Orsay, Cedex, France
[3] LSCE, UMR CEA/CNRS 1572, L'Orme des Merisiers CEA Saclay, 91191 Gif/Yvette cedex, France
[4] IFP Energies nouvelles, 1-4 avenue de Bois-Préau, 92852 Rueil-Malmaison, France
[5] Institut de Physique du Globe de Paris, Sorbonne Paris Cité, Université Paris Diderot, UMR 7154 CNRS, 75005 Paris, France.

Key points:

A new fluid inclusion analytical line with a productivity up to ten carbonate isotopic measurements per working day

A new reliable and accurate fluid inclusion analytical line for $\delta^{18}O$ and δD fluid inclusion analyses in carbonates

Fluid inclusion $\delta^{18}O$ of diagenetic cements agree, within 1 ‰, with the $\delta^{18}O$ independently derived from Δ_{47} measurements

Abstract

$\delta^{18}O$ and δD of fluid inclusions in carbonates provide insights into temperatures and fluid chemical compositions prevailing during the carbonate precipitation, however various analytical restrictions limit a wider application of this proxy. This paper presents a new fluid inclusions isotopic analytical line coupled to an online cavity ring-down spectrometer that increased the analytical productivity up to ten carbonate samples per working day. This efficiency allowed for the first time to assess the reliability a large set of water samples with size ranging from 0.1 to 1 μL. Good reproducibility ($\pm$ 0.5 ‰ for $\delta^{18}O$ and $\pm$ 2 ‰ δD; 1σ) is obtained for water quantity superior or equal to 0.3 μL and no evidence of memory effect is found. The line is further tested using two types of natural carbonates: (1) modern speleothems samples from caves for which $\delta^{18}O$ and δD values of drip water were measured and (2) diagenetic carbonates for which the $\delta^{18}O$ of the parent water were independently back-calculated from carbonate clumped isotope Δ_{47} measurements. Speleothem fluid inclusion values despite falling close to the Global Meteoritic Water Line are not always representative of the isotopic composition of the parent drip water. Results on diagenetic cements show that the $\delta^{18}O_{water}$ values measured in fluid inclusions agree, within 1 %, with the $\delta^{18}O_{water}$ independently derived from Δ_{47} measurements. Overall, this study confirms the reliability and accuracy of the developed analytical line for carbonate fluid inclusion analyses with a good reproducibility obtained for water quantity above 0.3 μL.

1. Introduction

Fluid inclusions are fluid-filled voids sealed within minerals that represent relicts of the paleo-water having precipitated the minerals (i.e. parent water). $\delta^{18}O$ and δD analyses of fluid inclusions can provide insights into temperatures and chemical conditions prevailing during the precipitation of carbonate minerals. While temperature, salinity, and pressure conditions at the time of fluid inclusion trapping can be deduced from micro-thermometric measurements on diagenetic carbonates (Goldstein and Reynolds 1994), $\delta^{18}O$ and δD composition of fluid inclusions is still technically challenging to measure in carbonates, mainly due to the small quantity of water extractable from the crushing of these minerals. Obtaining $\delta^{18}O$ and δD composition of diagenetic carbonate fluid inclusions would however have major scientific purposes such as a better characterization of the water origin and evolution in carbonate systems from both Earth surface (e.g. palaeosols or speleothems) and sub-surface (e.g. groundwaters). The $\delta^{18}O$ and δD analyses of fluid inclusions in diagenetic carbonates may provide information about chemical conditions prevailing in sedimentary units over the evolution of sedimentary basins. This would allow for a better characterization of past basin groundwaters, as well as their evolution during water/rock interactions over time. In speleothems (cave carbonate concretions), fluid inclusions preserve information of the isotopic composition of past cave drip waters; they are relics of past precipitations averaged over a period of few months to few years (Hendy et al., 1969; Genty et al., 2014). Combined with speleothem carbonates $\delta^{18}O$ analyses, $\delta^{18}O$ and δD of speleothem fluid inclusions can be used as a direct proxy for moisture source, amount history of precipitation (Schwarcz et al., 1976), and/or cave paleo-temperatures (which is close to the mean annual temperature outside the cave, assuming that an isotopic equilibrium state is reached (Mickler et al., 2004)).

$\delta^{18}O$ and δD compositions of speleothem fluid inclusions have been analyzed since the pioneering work of Schwarcz et al. (1976), but until recently, technics were imprecise, time-consuming, and very restrictive in term of sample quantity. Over the last decade, various analytical lines and set-up were used, all of them unique in their design (i.e. Dallai et al., 2004; Vonhof et al., 2006, 2007; Dublyansky and Spötl, 2009). Recent studies have presented laser spectroscopy (Cavity-Ring Down Spectroscopy (CRDS) PICARRO) as a valuable method to analyze simultaneously $\delta^{18}O$ and δD of speleothem fluid inclusions (Arienzo et al., 2013; Affolter et al., 2014; Uemura et al., 2016). Arienzo et al. (2013) were the first to develop an on-line analytical line coupled to a CRDS that allows the direct measurement of both $\delta^{18}O$ and δD on speleothem fluid inclusions. A speleothem calcite chip is crushed into a 115 °C heated line, which is entirely made of stainless steel. The crusher is a modified Nupro vacuum valve. They added an injection port to be able to analyse water standards. The water released by injection and crushing is carried *via* a carrier gas (dry Nitrogen) to an expansion volume. This expansion volume serves as reservoir to feed the CRDS analyzer. The main advantage of this line is that the volume, once isolated from the upstream part of the line, provides a continuous stable signal to be analyzed. For water samples of 0.5 μL or more, the precision of this analytical line is 0.4 ‰ for $\delta^{18}O$ and 1.1 ‰ for δD. The time needed to analyze a speleothem sample is in the range of 1 to 2 hours. The second analytical line, created by Affolter et al. (2014) is constantly under humid condition. A humid background of set H_2O concentration and known $\delta^{18}O$ and δD values is constantly flushed thought the line and analysed by the CRDS analyser. A humid background allows for the measurements of fluid inclusion waters to be performed close to the optimal water vapor concentration range of the PICARRO analyser (17,000 – 23,000 ppmv). Speleothem calcite chips are crushed using a hydraulic press. This line has the same injection port as Arienzo

et al. (2013) to enable manual injections of water samples. Fluid inclusion and injection waters are measured on top of the background line. This technic allows the PICARRO analyser to be more stable and gets rid of the memory effect. For water samples of 1 μL or more, the precision of this analytical line is 0.4 ‰ for $\delta^{18}O$ and 1.5 ‰ for δD, this precision decreases for smaller quantities of water. The time needed to analyze a speleothem sample is in the range of 2 to 5 hours. Uemura et al. (2016) developed a new highly sophisticated line resembling the Arienzo et al. (2013) design. They have however custom-made glass devices for the three main units, the crusher, injection port, and expansion chamber. Another difference with the Arienzo et al. (2013) line is the use of a cryogenic trap to collect the water released from the speleothem before diluting it in the expansion chamber. This new design permits low contents of water (50-260 nL) to be analyzed with a precision of 0.05 to 0.61 ‰ for $\delta^{18}O$ and 0 to 2.9 ‰ for δD. However, analysis time is 7 hours per sample. Thanks to those recent studies, potential of isotope measurements of fluid inclusion water is now fully recognized. However, various analytical limitations such as sample size restrictions or time consuming analysis are still making a wider application of this climate proxy difficult.

In this study we present a new analytical line based on both Arienzo et al. (2013) and Affolter et al. (2014) designs, named for the rest of the manuscript as the Miami and Bern lines, respectively. Our goal is to increase the productivity of the analytical line while keeping the quantity of needed water realized by crushing below 0.5 μL. Sample quantity is a critical parameter to ensure the possibility of analyzing (1) different types of natural carbonate samples, (2) carbonates with relatively low water content, and (3) several replicates of a single carbonate sample. We therefore assessed, for the first time, errors associated with sample sizes ranging from 0.1 to 1μl. This manuscript first describes technical aspects and design of this new

analytical line. A thorough assessment of the reliability of water sample measurements was then achieved to calculate the minimum fluid inclusion quantity needed to obtain reliable $\delta^{18}O$ and δD values. At last, we present results from natural carbonates samples: speleothems and diagenetic carbonates (calcites and dolomites).

2. Analytical line description

2.1. Material

A schematic of the line is presented in Figure 1; it includes three main units, a water vapor background generator section, an injection line permitting both water injections and crushing of carbonate material, and a bypass line. The entire line is continuously flushed with dry nitrogen gas and heated at a constant temperature of 130 °C with warming bands. The heated line, that is controlled at two different locations, is wrapped in aluminum foil to permit homogeneous heating conditions. The heating ensures the absence of cold spots (<100 °C) which could lead to the condensation of the water vapor. A layer of insulating cork material is added to protect the line from external environment and avoid heat loss.

Water vapor background generator

The water vapor background generator is similar to the one developed for the Bern line. The first component of the line is a water reserve containing an in-house water standard named BAFF. BAFF is a natural fresh water, collected in the Baffin Island (North of Canada). It was sampled in large enough quantity (about 30 L) to be used as an internal reference water standard of the GEOPS laboratory. BAFF was calibrated against internationals standards: Vienna Standard Mean Ocean Water scale (VSMOW), Greenland Ice Sheet Precipitation (GISP), and

Standard Light Antarctic Precipitation (SLAP). Analyses made on a mass spectrometer (IRMS Thermo Finnigan Delta Plus, equipped with an equilibrating bench), gave the following results: $\delta^{18}O$ = -15.42 ‰ ± 0.03 (1σ) (n=9); δD = -121.85 ‰ ± 0.86 (1σ) (n=6).

BAFF standard is extracted from the water reserve by a high precision peristaltic pump with planetary traction (ISMATEC # ISM945D). Water from the peristaltic pump is carried by a TYGON LMT-55 tubing (SCO0188T; ID: 0.13 mm and wall: 0.91 mm), to a fused silica capillary (IDEX Heath & Science FS-115; ID: 150 μm; wall: 360 μm; lengh: ~10 cm), to a vaporizer (an union tee: Swagelok # SS-200-3). The carrier gas arrives to the vaporizer from the upstream side of the union tee and the BAFF standard arrives thought the side. The fused silica capillary, carrying BAFF standard, slightly touches the wall of the union tee which instantaneously vaporized it and carried it downstream. A purge is added to the line to evacuate parts of the vaporized water. This purge consists of a 5 cm stainless steel capillary (1/16") attached to the line via a union tee (Swagelok # SS-200-3). Downstream of the purge is a mixing cavity that reduces the water pulses coming from the vaporizer and homogenizes the water vapor background. This mixing cavity consists of a 150 mL stainless steel cylinder (Swagelok 304L-HDF4-150-PD). The quantity of water vapor background going through the line is modified by increasing or decreasing the velocity of the peristaltic pump. A three ways valve (Swagelok SS-41GXS2) separates the water vapor background generator section from both the injection and bypass lines.

Injection line

The first component of the injection line is the syringe injection unit that is similar to both the Miami and Bern lines. It consists of a septum injection nut (Cluzeau Info Labo #

EN2SI) fixed to the line *via* a union tee (SS-200-3). A 1 μL syringe (SGE Analytical Sciences syringe) is used to inject water standards with quantities ranging from 0.1 to 1 μL. The second component is the crushing device (Figure 2) that consists of a modified vacuum valve (Swagelok #SS-4BG), in which the valve stern was taken apart from the valve body. The valve body was milled until obtaining a 1 cm diameter cavity. The stern cap was replaced by a custom-made stainless steel cylindrical hammer (see Figure 2 for details). To crush the sample, the valve stern is used as a power hammer, with the valve bellow leading to the crush of the carbonate sample by vertical pressure and vibrations. Similar to the Miami line, a 0.5 μm pore size (Swagelok SS-4F-05) in-line filter is inserted downstream from the crusher to prevent particles of carbonate to be transported to the PICARRO analyzer. A 75 ml expansion volume (Swagelok 304L-HDF4-75-PD) is added to buffer the water coming from injection or crushing. This volume tends to mimic the PICARRO vaporizer units used in the Bern line, without diluting the signal.

Bypass line

The bypass line consists of a 1/8" stainless steel tubing. In the Bern line the stabilization time after opening the line was around three hours. By switching to this bypass line, the PICARRO analyser remains under continuous humid flow when we open the crusher to insert carbonate samples which reduce considerably the stabilization time to about 10 min.

2.2. Protocol for analysis

For each analytical session a similar protocol is followed (1) the PICARRO analyzer is turned on, (2) the dry nitrogen flushing valve is open, and (3) the peristaltic pump is turned on. A quiescence time of half an hour is necessary to obtain a stable humid background. The

determined conditions for a stable humid background are based on the standard deviation values over five minutes: H_2O concentration $\pm$ 10 (1σ) ppmv, $\delta^{18}O \pm 0.2$ (1σ) ‰ and $\delta D \pm 4$ (1σ) ‰. Once these conditions are reached, six 0.3 μL injections of a combination of three certified water standards (-5‰; -8‰, ESKA, and MAZA; Table 1) are made. Those values are used as part of the daily calibration. Between each injection, a quiescence time of ~ 10 min is necessary to reach again background stabilization before the next injection. Once these water standard injections are done, the line set up is switched to the bypass line to insert the carbonate sample in the crusher unit. Once the carbonate sample is loaded, the incoming flux is switched back to the injection line. Another quiescence of ~ 15 min is necessary to remove all impurities and plausible water contamination at the surface of the sample and to obtain a stable humid background. Finally, the sample is manually crushed, to a fine powder. The water initially trapped as fluid inclusions is released, vaporized, and carried to the PICARRO analyzer for direct isotopic measurements. The line is switched to the bypass line to insert another carbonate sample in the crusher unit. At the end of the day six 0.3 μL injections of the same certified water standards analyzed at the beginning of the day are ran to complete the daily calibration. This analytical set up allows to analyze about 10 carbonate samples per day on a regular, 8 hours, work day (see Figure 3 for details).

2.3. Data analysis

The data analysis is based on the method developed by Affolter et al. (2014). The signal is a mix between the background water and the water sample injected or liberated during the crushing. The shape of the signal for one measure (for all three parameters, water concentration, $\delta^{18}O$, and δD) resemble an abrupt peak followed by a slow return to background conditions. We

need to integrate the product of the water amount and its isotopic value with regard to the background to calculate sample isotopic $\delta^{18}O$ and δD values. To reduce the analytical noise, a 20-points-rolling median is applied to the three variables. This step was not done by Affolter et al. (2014) since their PICARRO analyzer (L1102-i) gives one value averaged over twelve seconds of measurement while our PICARRO analyzer (L2120) gives one value averaged over two seconds. The deconvolution between the signal and the baseline is a simple integration over the duration of the mix, with removal of the baseline, following equation (1) and (2):

$$(1) \quad \delta^{18}O = \frac{\overline{[H_2O]} * \dfrac{\sum_i \left([H_2O]_i * \delta^{18}O_i \right)}{\sum_i [H_2O]_i} - \left([H_2O]_{background} * \delta^{18}O_{background} \right)}{\overline{[H_2O]} - [H_2O]_{background}}$$

$$(2) \quad \delta D = \frac{\overline{[H_2O]} * \dfrac{\sum_i \left([H_2O]_i * \delta D_i \right)}{\sum_i [H_2O]_i} - \left([H_2O]_{background} * \delta D_{background} \right)}{\overline{[H_2O]} - [H_2O]_{background}}$$

The trickier part is to select the duration of the integration, by finding an objective sample signal beginning and end. To determine the signal inflection point we use an objective criterion of $dH_2O(t)/dt \geq 10$ ppmv.s^{-1}. The end of the sample signal is set when $dH_2O(t)/dt \geq 0$ ppmv.s^{-1} over a period of nine consecutive values. We automated these calculi by developing a VBA application (https://github.com/MaxenceDuhamel/AUTOPEAK-PICARRO.git).

3. Calibration of the line using water standards

3.1. Determination of the optimal water background concentration

To test the optimal water background concentration, the same protocol as in Affolter et al. (2014) was followed. This test was made over the course of eleven different days from three different months (Table 2 and Figure 4). We varied the background water concentration from 2,000 to 24,000 ppmv and analyzed it over a period of three hours. Data acquired over the last 30 minutes were averaged and used as the value for the set background condition (Table 2 and Figure 4). For $\delta^{18}O$ values, the standard deviation is high for concentration below 7,000 ppmv and then become stable with a standard deviation of 0.2 ‰. For δD, the standard deviation also decreases in a nearly exponential profile with the increase in H_2O concentration. The slope of the decrease become smaller around 7,000 ppmv, and the standard deviation of the δD measurements stays below 4 ‰ until 24,000 ppmv. As for the H_2O concentration, the standard deviation is stable around 10 ppmv until 11,000 ppmv, and then starts to increase. In regards to those results, the water background concentration for routine measures was set to 8,000 ppmv (Figure 4, red squares).

3.2. Estimation of sample's water concentration

Various aliquot of water ranging from 0.1 to 1 µL (30 replicates for each aliquot) were injected to define the relationship between the quantity of water injected and the integrated water volume measured on the PICARRO analyzer (see section 2.3 water integration). A significant linear relationship is found between the quantity of water injected and the integrated water volume measured on the PICARRO (Figure 5). The equation derived from this linear regression: $7.436e-7\ (\pm 3.464e^{-9})\ x + 8.049\ (\pm 2.852e^{-3})\ (R^2 = 0.994$, significant at 99%) is used to determine the quantity of water released during carbonate sample crushing procedure.

3.3. Calibration of the instrument

Measured raw isotopic data coming from the instrument need to be converted into VSMOW scale. Four laboratory standards waters (-5‰, -8‰, ESKA, and MAZA see Table 1), previously calibrated against VSMOW, GISP, and SLAP, are used to perform the isotopic calibration of the instrument (Table 3 top panel and Figure 6). The range of the calibration is -1.18 to -13.96 ‰ for $\delta^{18}O$ and -100.15 to 1.28 ‰ for δD, spanning the entire range of isotopic values measured in fluid inclusions from natural carbonate samples. For each calibration curve presented in Figure 6, at least three replicates of 0.5 μL of laboratory standards were measured (Table 3 top panel). The mean calibrations (average of the five daily ones, Table 4) are y = 0.979 (± 0.005) * measured $\delta^{18}O$ + 1.371 (± 0.049) (R^2 = 0.999, significant at 99%) and y = 0.967 (± 0.004) * measured δD – 1.535 (±0.261) (R^2 = 0.999, significant at 99%). The 99 % confidence interval per standards, following a Student t test, range from 0.15 to 0.28 ‰ for $\delta^{18}O$ and from 0.79 to 1.71 ‰ for δD (Figure 6.C. and D.). These mean calibrations are used to correct both water injections and carbonate fluid inclusion water analyses. Daily calibrations are systematically compared to these mean calibrations to evaluate a potential drift of the instrument. Over the period of one year no significant drift was observed.

Additional certified laboratory standards waters (-30‰, NAN, DOMEC, and -10‰) were analyzed and plotted on top of the mean calibration curves to test the validity of these calibration equations for out of range water standards (Table 3 bottom panel and Figure 6.C. and D.). Each of these standards fall on the calibration lines, validating the linearity of the regressions which will allow to correct out of calibration-range sample values. To assess the memory effect of our line, five samples of MAZA were injected followed by five of DOMEC, two standards with very

different isotopic composition (Table 1). The mean values of the first two DOMEC values is not statistically different than the mean of the last two ones. We therefore concluded that there is no evidence of memory effect in our system (similar as Affolter et al., 2014).

4. Water sample reproducibility test

We document the accuracy and precision of the line by doing replication measurements of a laboratory water standard named DIDO2. It is a tap water, demineralized, and calibrated against VSMOW, GISP, and SLAP. DIDO2 analyses made on a mass spectrometer (IRMS Thermo Finnigan Delta Plus, equipped with an equilibrating bench), gave $\delta^{18}O$ = -7.30 ‰ ± 0.04 (1σ); δD = -49.91 ‰ ± 0.64 (1σ) (n=7). 30 replicates of different aliquots of DIDO2 ranging from 0.1 to 1 μL at a 0.1 μL increment were analysed (Figure 7). This is the first time such experiment was completed owing to the fact that it has been time consuming on previous analytical line designs. We used a bootstrap method to calculate the confidence interval of the mean. For 3% test over 1,000 iterations, mean $\delta^{18}O$ and δD values are not statistically different for injected volumes ranging from 0.3 to 0.8 μL. Standard deviation of the difference between the certified values and the measured values for a given injected volume are presented in Figure 7 (Bottom). For injection volume above or equal to 0.2 μL, the standard deviation for $\delta^{18}O$ reaches the acceptable value of 0.5 ‰. For δD, acceptable value of 2 ‰ is reached for injected volumes above or equal to 0.3 μL. This test indicates that our line has a good $\delta^{18}O$ and δD reproducibility for sample size above 0.3 μL.

5. Isotopic composition of fluid inclusions from natural carbonate samples

To validate the reliability of our analytical line, two different types of natural carbonate samples are analyzed: (1) modern speleothem samples from caves for which $\delta^{18}O$ and δD composition of drip water are known. It is commonly assumed that isotopic composition of speleothem fluid inclusions reflects the isotopic composition of the parent drip water, itself closely linked to rainfall variability (Genty et al., 2014); and (2) diagenetic carbonates for which the $\delta^{18}O$ of the mineralizing waters were independently back-calculated by combining clumped isotope (Δ_{47}) temperatures and $\delta^{18}O$ values of the carbonate (Mangenot et al., 2017, 2018). All the fluid inclusion isotopic values from carbonate samples are presented in Table 5.

5.1. Speleothems

Sample sites description

Speleothems used in this study come from two different locations in Northern Europe: Sweden (K13) and Belgium (HanGril). No petrography analyses were done due to the small quantity of calcite available for analyses.

K13 stalagmite comes from the Korallgrottan Cave, North West of Sweden, in the Caledonian mountain range (64° 53'16" N; 14° 9'30" E) located 540 to 600 m above sea level (Sundqvist et al. 2007). K13 is a 7.7 cm long stalagmite that grew mainly between 10.6 ky to 6.9 ky, with a last short growth period around 2 ky (K. Holmgren and H. Sundqvist, unpublished data). Calcite samples for fluid inclusion analyses were taken at the top of the stalagmite (the first 5 mm). We assume that the isotopic signal of the input water (rainfall and dripping water) did not change significantly over the last 2 ky, therefore, samples taken at the top of the stalagmite (from ~2 ky ago) should be representative of modern day values. Korallgrottan cave stalactite drip water was collected by H. Sunqvist and K. Holmgren during a monitoring

campaign between October 2013 and November 2014. Isotopic values of cave drip water feeding the stalagmite are $\delta^{18}O$ = -11.95 ± 0.13 ‰ (1σ) and δD = -85.03 ± 0.77‰ (1σ) (n=9) (Sunqvist et al., 2007; Table 7).

HanGril samples come from the Han-sur-Lesse Cave, South of Belgium (50 °7'16" N; 5 °11'46" E) located 160 m above sea level. Both HanGrilA and HanGrilB are modern calcite that grew between 1995 to 2012. HanGrilB grew on artificial iron shelves positioned on the floor of the "Salle du Dôme", and HanGrilA grew on an artificial tile that was positioned on the horizontal part of the iron shelf. Regular measurements of cave drip water from a dripping site located nearby HanGrilA and HanGrilB speleothems, were made at a frequency of one sample a month in 2011 and two samples a month in 2012. Isotopic values of cave drip water are $\delta^{18}O$ = -7.65 ± 0.07 ‰ (1σ) and δD = -50.10 ± 0.39 ‰ (1σ) (n = 36) (Van Rampelbergh et al., 2014; Table 7). A water sample from the drip water feeding HanGrilA/B deposits was collected in July 2012 giving values close to the aforementioned measurements ($\delta^{18}O$ = -7.37 ‰ and δD = -49.15 ‰). Cave drip water isotopic measurements can therefore be used as reliable source of information on speleothem parent water.

Sample fluid inclusion concentrations

The relationship between the weight of the speleothem sample and the quantity of the water released during the crushing is examined (Figure 8A., B, and C). The weight of speleothem chips varies from 0.04 to 0.84 g, with the amount of water released between 0.09 to 1.12 µL. We observe a positive linear relationship between the amount of speleothem crushed and the quantity of water released for both K13 and HanGrilB samples, with Pearson correlation values of 0.95 and 0.90, respectively (both significant at 99 %). We find however, no significant

relationship between the sample weight and the amount of water released for HanGrilA samples. This result points to a heterogeneous distribution of fluid inclusions in stalagmite samples as already presented in Affolter et al. (2014) and Meckler et al. (2015).

Isotopic measurements

Isotopic fluid inclusion $\delta^{18}O$ and δD values from K13, HanGrilA, and HanGrilB are presented in Table 5 and Figure 8.D. Most of the fluid inclusion values are closed to the Global Meteoritic Water Line (GWML; Craig, 1961), which indicates that enclosed fluid inclusions were not influenced much by evaporation and should therefore reflect isotopic composition of parent drip water. The only out of range value (Figure 8.D. black circle) is from a sample that released a water volume below 0.1 μL, and could not be considered as reliable (see section 4). Mean fluid inclusions $\delta^{18}O$ and δD for each speleothem, are plotted with the isotopic composition of their parent drip water (Figure 8.E). Recent studies found that local drip water values are slightly offset towards more negative $\delta^{18}O$ values relative to the local or global meteoritic water line (Genty et al., 2014; Meckler et al., 2015). This offset has been attributed to condensation on cave walls (Genty et al., 2014). In this study, local drip water from both Korallgrottan and Han-sur-Lesse caves (Figure 8.E.) fall on the GMWL. This demonstrates that the signals are of meteoric origin and that no fractionation through evaporation has occurred.

Isotope ratio in fluid inclusions from K13 samples are similar (within 1σ) to the isotopic composition of the parent drip water (Figure 8.E). This indicates that no fractionation occurred and consequently fluid inclusions in this speleothem is reliable and give isotopic values close to past rainfall. This is not the case for both HanGrilA and HanGrilB samples. Results from both speleothem (HanGrilA and HanGrilB) fluid inclusions are similar within 1σ, but are significantly

different from the parent drip water (Figure 8.E.). Both δ^{18}O and δD fluid inclusion values are different from the isotopic composition of the parent drip water, cancelling out a hypothetical exchange between calcite and fluid inclusion water after its formation. Fluid inclusions in both HanGrilA and HanGrilB samples might not be in equilibrium with their parent drip water. Another possible reason for the isotopic composition of an inclusion being different from the parent water is that the inclusion had leaked. Both HanGrilA and HanGrilB are speleothem deposited on a flat tile. Those samples might not be representative of natural growth conditions of stalagmites as already suggested by Labuhn et al. (2015), for similar cave deposits.

Section 4 determines that good δ^{18}O and δD reproducibility are achieved for sample size above 0.3 μL; it is also the case for crushed speleothem samples. While the mean isotopic values between all the crushed samples and the samples that released more than 0.3 μL of water are not statistically different, the standard deviation and therefore the reproducibility varies. For samples that released more than 0.3 μL, the reproducibility is about 0.5 ‰ for δ^{18}O and 2 ‰ for δD while it is much higher for the other ones, validating 0.3μl as the minimum water quantity to obtain robust isotopic fluid inclusions measurements.

5.2. Diagenetic carbonates

Samples description

δ^{18}O and δD of fluid inclusions were analysed in four calcitic and one dolomitic pore-filling cements, precipitated in a Middle Jurassic carbonate unit of the Paris basin. Most of the investigated samples (BEBJ8, VPU4, VPU9, and RN21) were collected at 1700-1800 m depth (basin depocenter) from a mineral paragenetic sequence already established by Mangenot et al. (2018) that consists of: (1) a first calcite cement named Cal1 (crystals 100 μm to 3mm), (2) a

saddle dolomite cement, named Dol1 (crystals 200 μm to 2mm), (3) a second calcite cement, named Cal2 (crystals 100 μm to 1mm). A fourth sample (BUF4) was collected at the exposed southern margin of the basin (Burgundy outcrops) and consists of a vein filling Cal3 (crystals 500 μm to 5mm). Except for BUF4, all the cements were previously investigated in term of petrography, fluid inclusion microthermometry and stable isotope geochemistry ($\delta^{13}C$, $\delta^{18}O$, Δ_{47}) by Mangenot et al. (2017) and Mangenot et al. (2018). Petrographic and microthermometric analyses of fluid inclusions revealed that all samples host primary and co-genetic populations of fluid inclusions which did not undergo any post-entrapment modifications (e.g. leakage, thermal re-equilibration, or refilling processes). The range of homogenization temperatures found for Cal1, Cal2 and Dol1 fluid inclusions are clustered at 63 ± 11°C, 80 ± 10°C, and 98 ± 5°C, respectively (see Mangenot et al., 2017). Complementary stable isotope analyses ($\delta^{13}C$, $\delta^{18}O$, Δ_{47}) confirmed that these three generations of cements precipitated at distinctive temperatures and from paleo-waters with different geochemistry. Published Δ_{47} compositions and associated $T\Delta_{47}$ temperatures for Cal1, Dol1, and Cal2 samples, calculated using the universal calibration of Bonifacie et al. (2017) as well as the additional data for BUF4 sample, are compiled in Table 8. By combining clumped isotopes temperatures ($T\Delta_{47}$) and $\delta^{18}O$ values of the carbonate, the $\delta^{18}O$ of the parent water ($\delta^{18}O_{water}$) can be reconstructed, here using the fractionation value of oxygen isotopes between the carbonate and water of O'Neil et al. (1969) for calcite and Horita et al. (2014) for dolomite. Calculated $\delta^{18}O_{water}$ values and their uncertainties are presented in Table 8.

Fluid inclusion measurements

   $\delta^{18}O$ composition of fluid inclusions were measured in the same cement specimens in order to be directly compared to the $\delta^{18}O_{water}$ values deduced from Δ_{47} data (Table 8). Fluid

inclusion mean $\delta^{18}O$ are: 2.5 ± 1.1 ‰ (n = 4) for BEBJ8, 2.4 ± 1.1 ‰ (n = 4) for VPU9, 0.6 ± 1.6 ‰ (n = 2) for VPU4, -3.1 ± 2.8 ‰ (n = 2) for RN21, and -6.6 ± 0.5 ‰ (n = 3) for BUF4. Fluid inclusion δD values are: -18.9 ± 5.4 ‰ (n = 4) for BEBJ8, -18.6 ± 3.1 ‰ (n = 4) for VPU9, -17.4 ± 1.9 ‰ (n = 2) for VPU4, -44.2 ± 7.9 ‰ for RN21 (n = 2) and -31.2 ± 1.4 ‰ (n = 3) for BUF4 (Table 8). Uncertainties, reported as one standard deviation of the mean, are quite variable for $\delta^{18}O$ measurements (between 0.5 and 2.8 ‰), and mostly dependant to the carbonate sample size and fluid inclusion abundance.

The cross-plot between $\delta^{18}O$ and δD is not reported for diagenetic samples as we do not expect their $\delta^{18}O$ and δD composition to fall on the GLWL. However, relationships between $\delta^{18}O$ values measured in fluid inclusions and $\delta^{18}O_{water}$ back-calculated from Δ_{47} data on the same mineral can be directly compared and evaluated. This relationship is plotted in Figure 9 with the 1:1 line marked.

Although each analytical technique comes with their own working hypotheses and uncertainties, all the results are remarkably consistent for a total range of variation between -6‰ to +2‰. Notably, $\delta^{18}O$ values measured in fluid inclusions agree within ~ 1‰ with $\delta^{18}O_{water}$ values calculated from $T\Delta_{47}$ and carbonate $\delta^{18}O$ data of the host-mineral. This very good agreement suggests that both methods reproduce realistic $\delta^{18}O_{water}$ values of the water from which natural carbonates precipitated, and confirms three important points: i) an independent cross-validation of both methods from natural samples that experienced a complex burial history (Mangenot et al. 2018), ii) the absence of substantial isotopic water-rock interaction between the host carbonate and the fluid inclusion water since mineral precipitation. Given the relatively low water to rock ratio between the microvolumes of fluid inclusion water and the carbonate matrix, such isotopic exchanges would likely have changed the isotopic composition of the fluid

inclusion water, without changing the $\delta^{18}O_{water}$ back-calculated from the mineral, iii) the primary

and co-genetic natures of fluid inclusions within all of the investigated samples which did not

undergo post-entrapment modifications (e.g. no mixing of different fluid inclusions populations

and no leakage, thermal re-equilibration or and/or refilling processes).

6. Summary and conclusions

This study presents a newly designed analytical line dedicated to the analyze of fluid

inclusion $\delta^{18}O$ and δD in carbonate samples. The design is based on two previously developed

line, the Miami line (Arienzo et al., 2013) and the Bern line (Affolter et al., 2014) and allow to

increase the productivity up to ten carbonate samples per working day, while being able to keep

the sample size yield below 0.5 μL.

We assessed for the first time the reliability of such line by analyzing a large set of water

samples of different size ranging from 0.1 to 1.2 μL. The findings indicated that this newly

designed line has a good $\delta^{18}O$ and δD reproducibility for sample size above 0.2 μL and 0.4 μL,

respectively. We further tested the line using two type of carbonates samples, speleothems and

diagenetic carbonate. For the speleothem samples, we looked at the relationship between the

weight of the sample and the quantity of the water released during the crushing. The result points

to a heterogeneous distribution of fluid inclusions in stalagmite samples as already presented in

Affolter et al. (2014) and Meckler et al. (2015). We compared speleothem fluid inclusion $\delta^{18}O$

and δD obtained on this new analytical line with isotopic composition of the parent drip water.

Results suggest that the analytical line is valid for speleothem fluid inclusion analyses. However,

isotopic composition of fluid inclusion and parent drip water are not always coherent, pointing

out the need of combining both water drip and fluid inclusions analyses to assess the potential of

a stalagmite for paleoclimate study. An independent comparison between $\delta^{18}O$ water values directly measured in fluid inclusions and the $\delta^{18}O$ water indirectly back-calculated from Δ_{47} composition of diagenetic carbonates revealed that both methods reproduce realistic $\delta^{18}O_{water}$ values, with typical uncertainties of ± 1‰. Such results are promising for future application of $\delta^{18}O$ and δD measurements of fluid inclusions from diagenetic carbonates aiming to evaluate the chemical evolution of ancient groundwaters in sedimentary basins.

Reference List:

Affolter, S., D. Fleitmann, and M. Leuenberger, 2014: New on-line method for water isotope analysis of speleothem fluid inclusions using laser absorption spectroscopy (WS-CRDS).

Clim. Past Discuss, **10**, 429–467, doi:10.5194/cpd-10-429-2014.

Arienzo, M. M., P. K. Swart, and H. B. Vonhof, 2013: Measurement of $\delta^{18}O$ and δ^2H values of fluid inclusion water in speleothems using cavity ring-down spectroscopy compared with isotope ratio mass spectrometry. *Rapid Commun. Mass Spectrom*, **27**, 2616–2624, doi:10.1002/rcm.6723.

Bonifacie, M., D. Calmels, J. M. Eiler, J. Horita, C. Chaduteau, C. Vasconcelos, P. Agrinier, A. Katz, B. H., Passey, J. M. Ferry, and J. J. Bourand, 2017: Experimental calibration of the dolomite clumped isotope thermometer from 25 to 350°C, and implications for the temperature estimates for all (Ca, Mg, Fe) CO_3 carbonates digested at high temperature. *Geochimica et Cosmochimica Acta*, **200**, 255-279, doi: 10.1016/j.gca.2016.11.028

Craig H., 1961, Isotopic variations in meteoric waters, Science, **133**, 1702-1703, doi:10.1126/science.133.3465.1702

Dallai L., L. Lucchini, Z.D. Sharp, 2004: Techniques for stable isotope analysis of fluid and gaseous inclusions, *Handbook of Stable Isotope Analytical Techniques*, de Groot P. (ed). Elsevier: Amsterdam, 62-77

Dublyansky Y. V., and C. Spötl, 2009: Hydrogen and oxygen isotopes of water from inclusions in minerals: design of a new crushing system and on-line continuous-flow isotope ratio mass spectrometric analysis. *Rapid Commun. Mass Spectrom*, **23**, 2605–2613, doi:10.1002/rcm.4155.

Genty, D., I. Labuhna , G. Hoffmann, P. A. Danis, O. Mestre, F. Bourges, K. Wainer, M. Massault, S. Van Exter, E. Régnier, Ph. Orengo, S. Falourd, and B.Minster, 2014: Rainfall and cave water isotopic relationships in two South-France sites. *Geochimica et Cosmochimica Acta*, **131**, 323–343, doi:10.1016/j.gca.2014.01.043.

Goldstein, R., and J. Reynolds, 1994: Systematics of Fluid Inclusions. SEPM Short Course Notes 31, 188, doi: 10.2110/scn.94.31

Hendy, C. H., 1971: The isotopic geochemistry of speleothems—I. The calculation of the effects of different modes of formation on the isotopic composition of speleothems and their applicability as palaeoclimatic indicators. *Geochimica et Cosmochimica Acta*, **35**, 801–824, doi:10.1016/0016-7037(71)90127-x.

Henkes, G. A., B. H. Passey, A. D. Wanamaker, E. L. Grossman, W. G. Ambrose, and M. L. Carroll, 2013: Carbonate clumped isotope compositions of modern marine mollusk and brachiopod shells. *Geochimica et Cosmochimica Acta*, **106**, 307–325, doi: 10.1016/j.gca.2012.12.020

Horita, J., 2014: Oxygen and carbon isotope fractionation in the system dolomite–water–CO2 to elevated temperatures. *Geochimica et Cosmochimica Acta*, **129**, 111–124. doi: 10.1016/j.gca.2013.12.027

Labuhn, I., D. Genty, H. Vonhof, C. Bourdin, D. Blamart, E. Douville, J. Ruan, H. Cheng, R. Lawrence Edwards, E. Pons-Branchu, and M. Pierre, 2015: A high-resolution fluid inclusion $\delta^{18}O$ record from a stalagmite in SW France: modern calibration and comparison with multiple proxies. *Quaternary Science Reviews*, **110**, 152–165, doi:10.1016/j.quascirev.2014.12.021.

Mangenot X., M. Bonifacie, M. Gasparrini, A. Goetz, C. Chaduteau, M. Ader, and V. Rouchon (2017). Coupling Δ_{47} and fluid inclusion thermometries on carbonate cements to precisely reconstruct the temperature, salinity and $\delta^{18}O$ of circulating paleowater in sedimentary basins. *Chemical Geology*, 472, 44-57, doi: 10.1016/j.chemgeo.2017.10.01

Mangenot X., M. Gasparrini, M. Bonifacie, V. Rouchon, M. Bonifacie (2018). Basin scale

thermal and fluid-flow histories revealed by carbonate clumped isotopes (Δ_{47}) - Middle Jurassic of the Paris Basin. *Sedimentology*, 65, 123-150, doi: 10.1111/sed.12427

Meckler A. N., S. Affolter, Y. V. Dublyansky, Y. Krüger, N. Vogel, S. M. Bernasconi, M. Frenz, R. Kipfer, M. Leuenberger, C. Spötl, S. Carolin, K. M. Cobb, J. Moerman, J. F. Adkins, and D. Fleitmann, 2015: Glacial-interglacial temperature change in the tropical West Pacific: A comparison of stalagmite-based paleo-thermometers. *Quaternary Science Reviews*, 1–28, doi:10.1016/j.quascirev.2015.06.015.

Mickler, P. J., J. L. Banner, L. Stern, Y. Asmerom, R. L. Edwards, and E. Ito, 2004: Stable isotope variations in modern tropical speleothems: Evaluating equilibrium *vs.* kinetic isotope effects. *Geochimica et Cosmochimica Acta*, **68**, 4381–4393, doi:10.1016/j.gca.2004.02.012.

O'Neil, J.R., 1969: Equilibrium and nonequilibrium oxygen isotope effects in synthetic carbonates. *Geochimica et Cosmochimica Acta*. 61, 3461–3475, doi: 10.1016/S0016-7037(97)00169-5

Schwarcz, H. P., R. S. Harmon, and P. Thompson, 1976: Stable isotope studies of fluid inclusions in speleothems and their paleoclimatic significance. *Geochimica et Cosmochimica Acta*, **40**, 657–665, doi:10.1016/0016-7037(76)90111-3.

Sundqvist, H. S., J. Seibert, and K. Holmgren, 2007: Understanding conditions behind speleothem formation in Korallgrottan, northwestern Sweden. *Journal of Hydrology*, **347**, 13–22, doi:10.1016/j.jhydrol.2007.08.015.

Uemura, R., M. Nakamoto, R. Asami, S. Mishima, M. Gibo, K. Masaka, C. Jin-Ping, C-C. Wu, Y-We. Chang, and C-C. Shen, 2016: Precise oxygen and hydrogen isotope determination in nanoliter quantities of speleothem inclusion water by cavity ring-down spectroscopic techniques. *Geochimica et Cosmochimica Acta*, **172**, 159–176,

doi:10.1016/j.gca.2015.09.017.

Van Rampelbergh, M., S. Verheyden, M. Allan, Y. Quinif, E. Keppens, and P. Claeys, 2014: Monitoring of a fast-growing speleothem site from the Han-sur-Lesse cave, Belgium, indicates equilibrium deposition of the seasonal $\delta^{18}O$ and $\delta^{13}C$ signals in the calcite. *Climate of the Past*, 10, 1871–1885, doi:10.5194/cp-10-1871-2014.

Vonhof, H. B., M. R. van Breukelen, O. Postma, P. J. Rowe, T. C. Atkinson, and D. Kroon, 2006: A continuous-flow crushing device for on-line δ^2H analysis of fluid inclusion water in speleothems. *Rapid Commun. Mass Spectrom*, **20**, 2553–2558, doi:10.1002/rcm.2618.
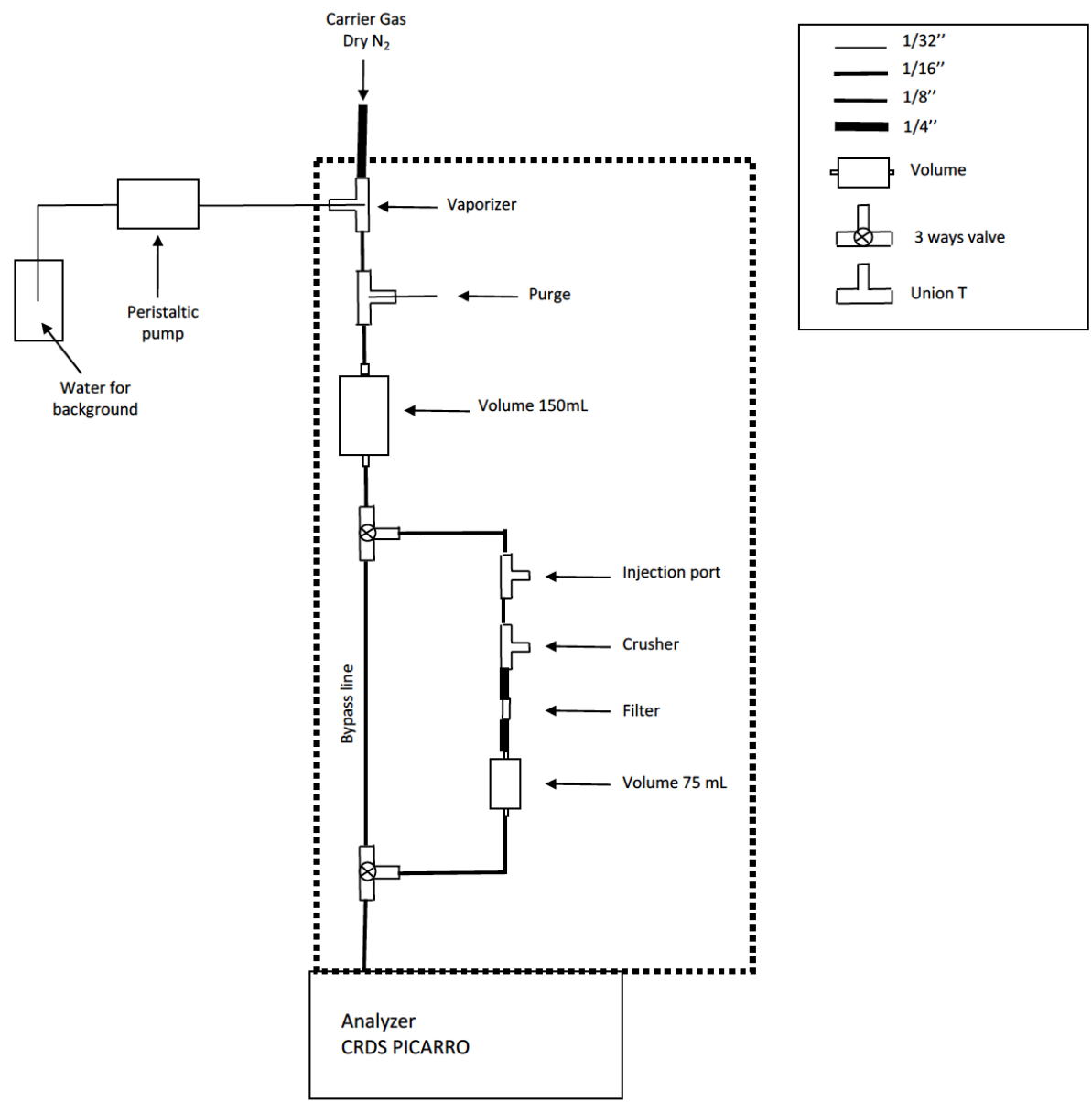
Figure 1: Schematic of the line which includes three main sections: a water vapor background generator section, an injection line permitting both water injections and crushing of carbonate material, and a bypass line. The part of the line heated at 130°C is delimited by the dotted square.
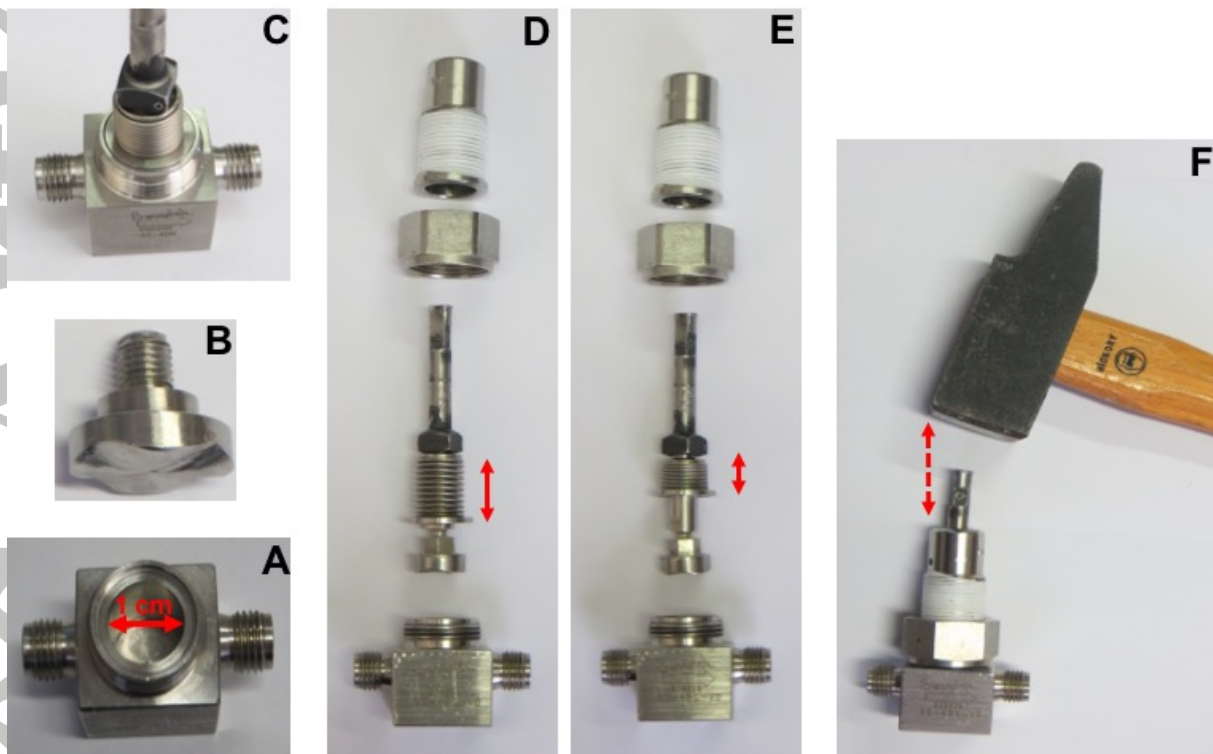
Figure 2: Different sections of the crushing device: A. The modified vacuum valve body milled to obtain a 1 cm diameter cavity, B. The modified valve stern cap used as a power hammer, C. The valve body and valve stern are sealed with airtight metallic-metallic connexion using metallic washer, D. and E. present the valve bellow before (D) and after (E) the crush, F. Picture presenting the vertical movement of the hammer hammering the top of the valve stern.
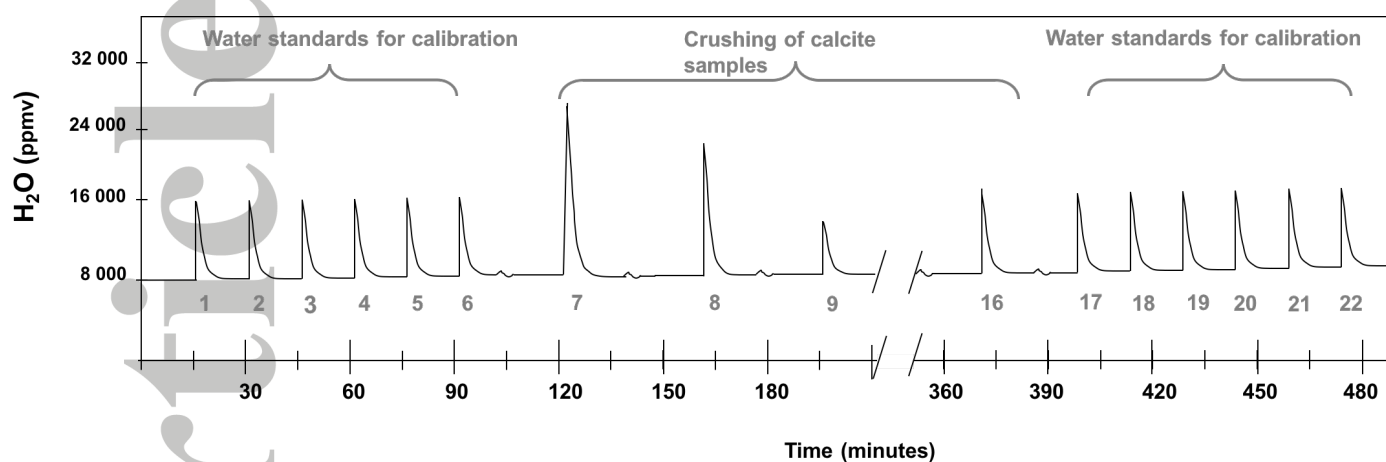
Figure 3: Schematic of water vapour evolution over the course of a regular analysing day. Peaks 1 to 6, are 0.3 μL injections of water standards for calibration MAZA (1, 2), -5‰ (3, 4), and -8‰ (5, 6). Peaks 7 to 16 corresponds to the released fluid inclusion water after calcite crushing. Peaks 17 to 22, are 0.3 μL injections of water standards for calibration MAZA (17, 18), -5‰ (19, 20), and -8‰ (21, 22).
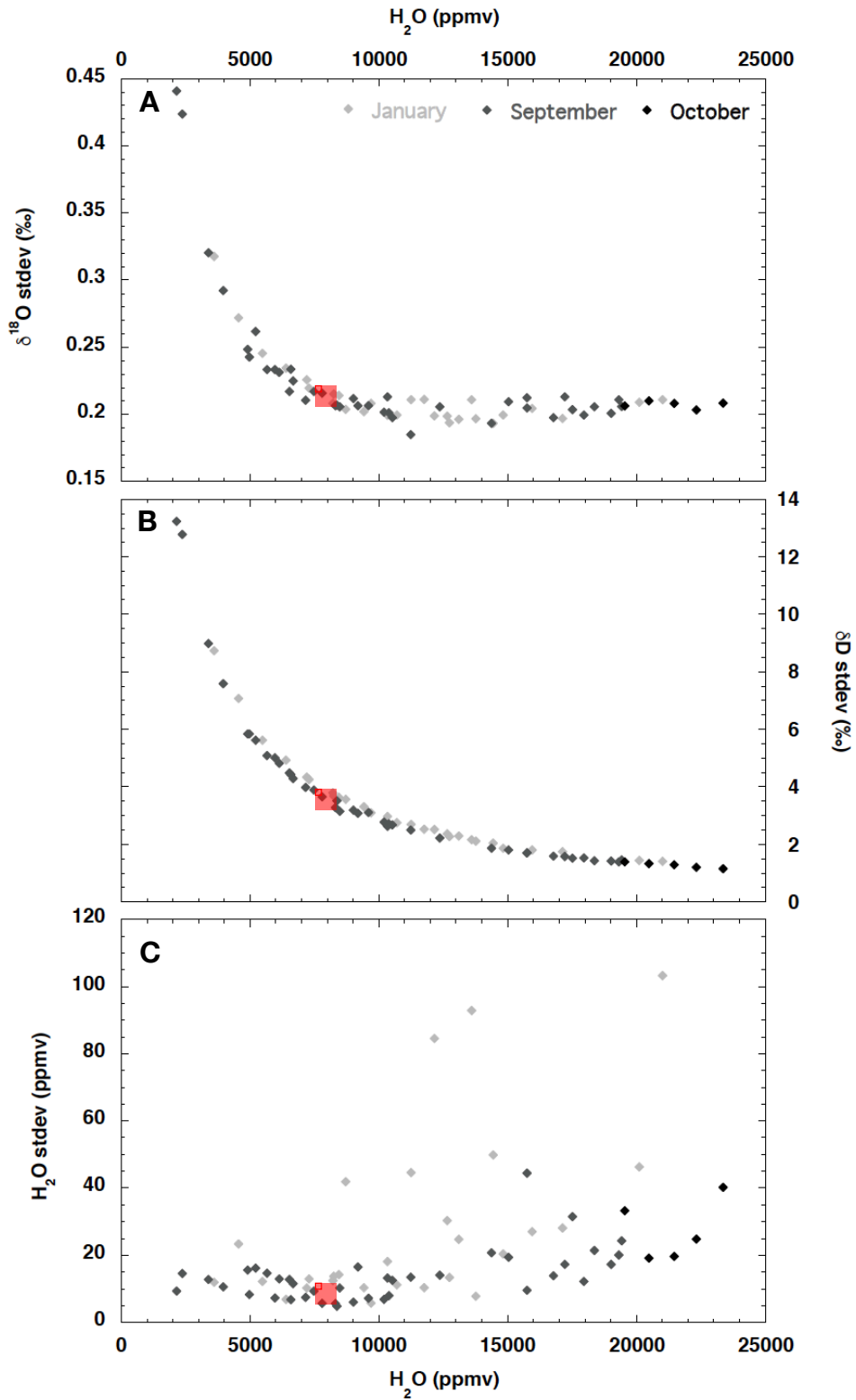
Figure 4: Water background stability. Each point corresponds to the standard deviation of A. $\delta^{18}O$, B. δD, and C. the water concentration (H_2O). Each set background was analyzed over a period of three hours and we averaged the data over the last 30 minutes. Red squares correspond to the background values chosen.
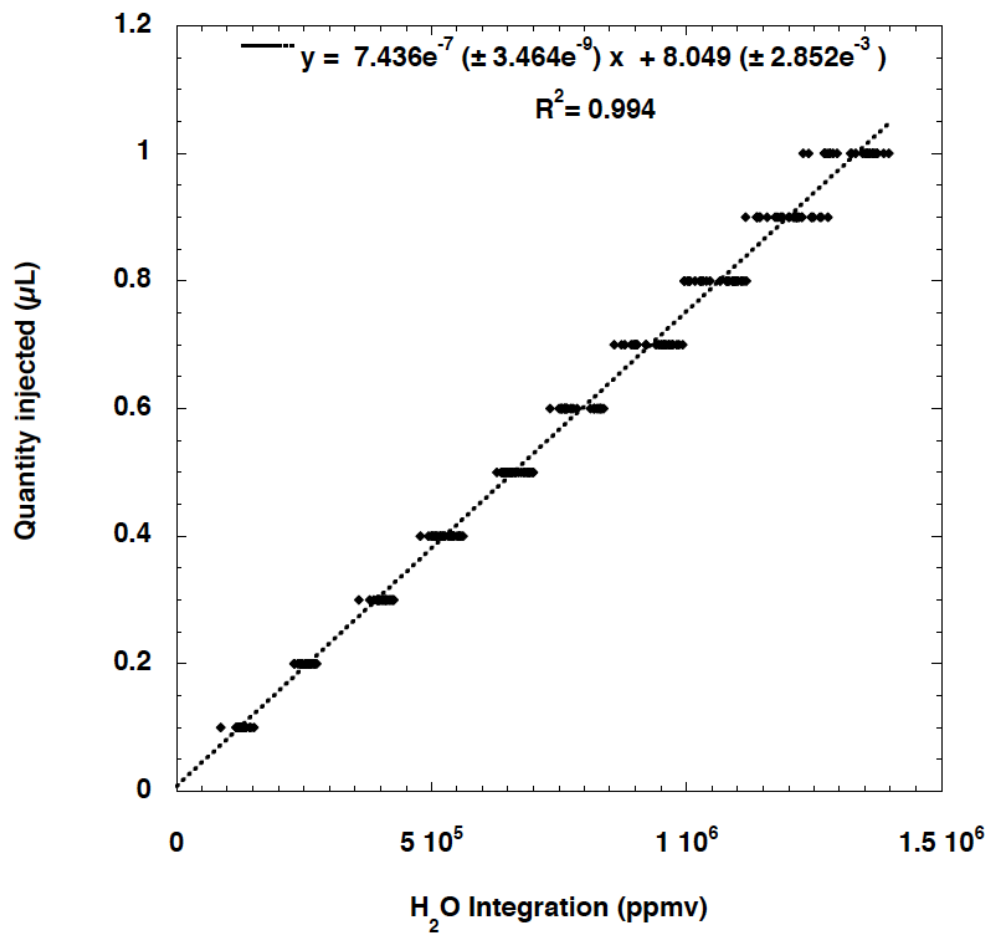
Figure 5: Linear regression between the quantity of water injected and the sample signal water amount integrated over the duration of the water peak.
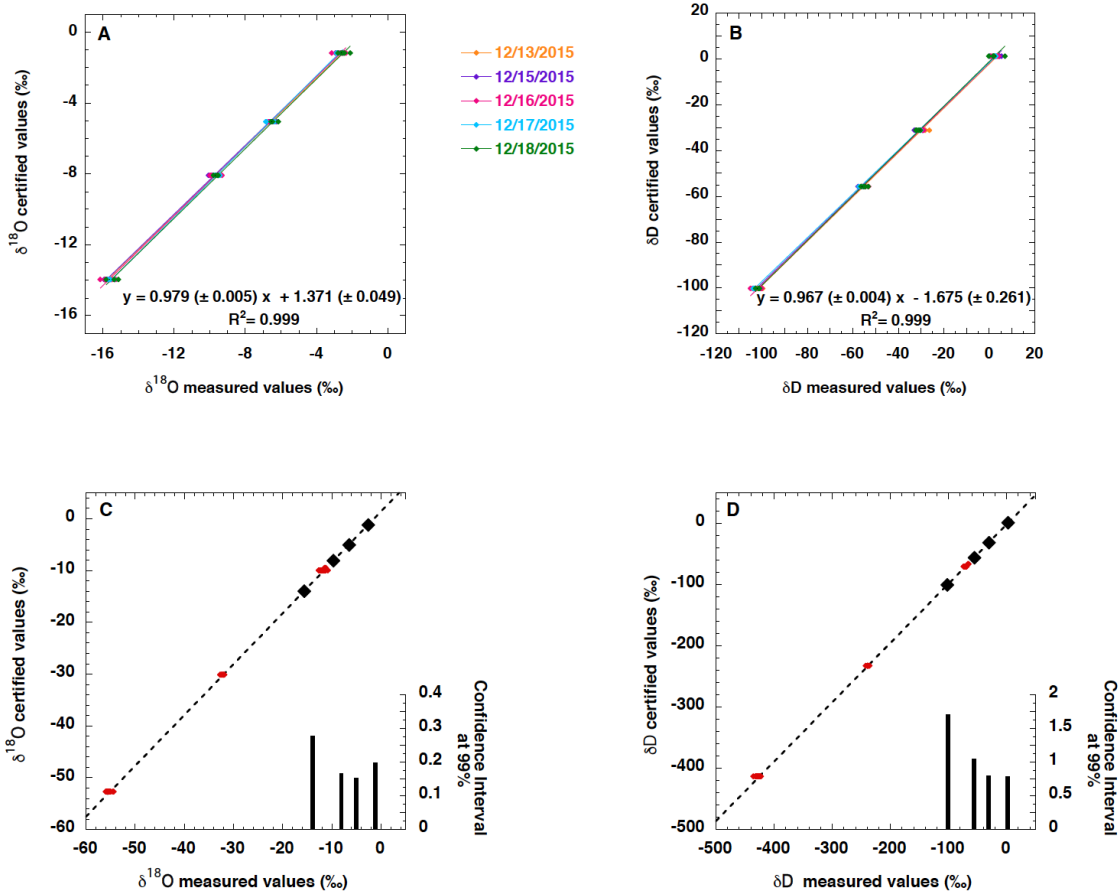
Figure 6: A. and B. Values of four 0.5 µL injections of laboratory standard (-5‰, -8‰, ESKA, and MAZA) over different days. The averaged calibration equation is represented in each plot. C. and D. Mean values for the calibration and confidence interval at 99 % for each point of calibration. The red dots are other laboratory standards (DOMEC; NAN; -10 ‰; -30 ‰; Table 1) analyzed to test the validity of the calibration for out of range water standards.
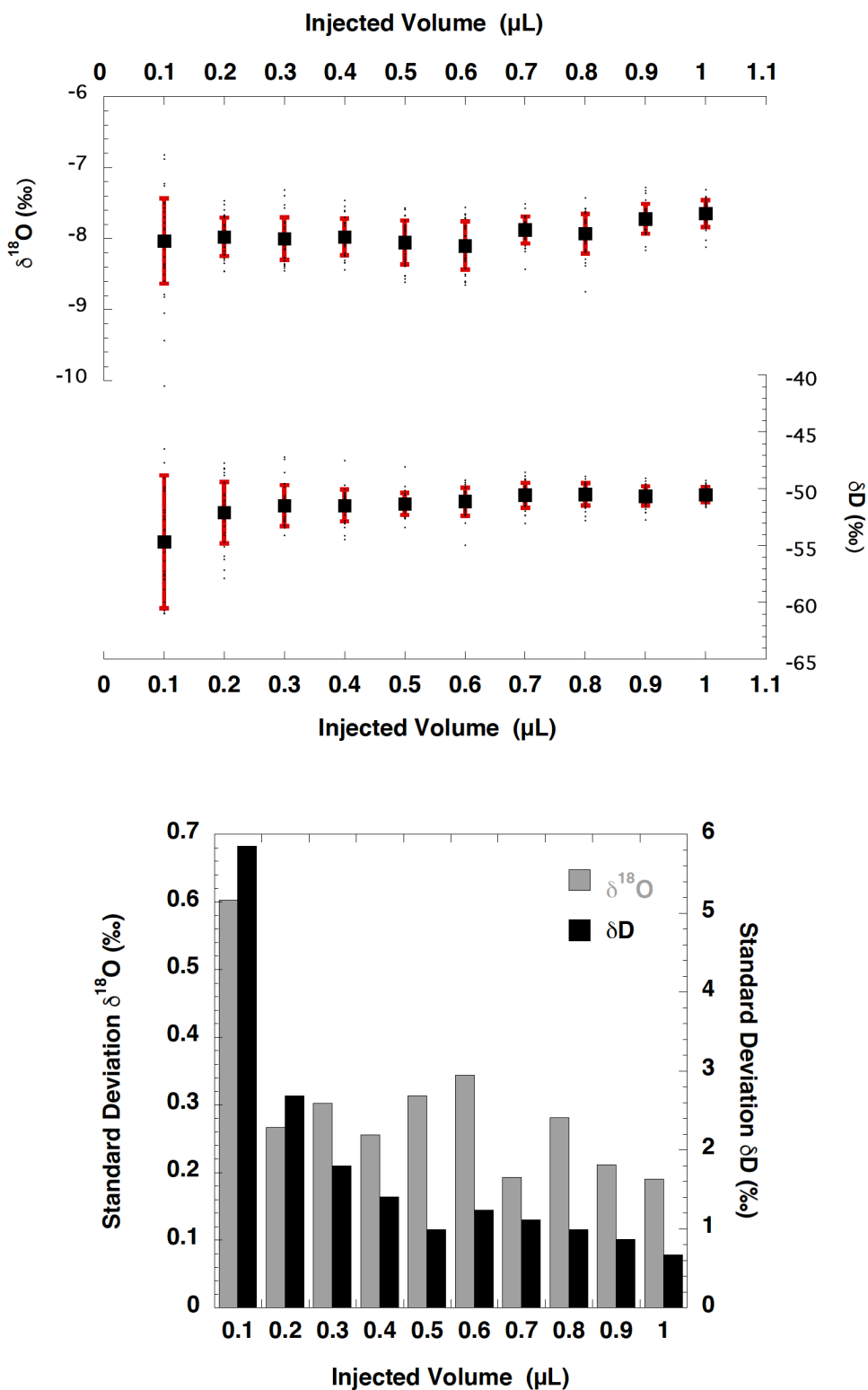
Figure 7: Top panel: $\delta^{18}O$ and δD values of 30 injections per injected volumes of DIDO2 (laboratory water standard) are plotted (black dots). Their means (black squares) and standard deviations (red lines) are presented. Bottom panel: Standard deviation of the difference between the certified values and the measured values for given injected volumes for both $\delta^{18}O$ (grey) and δD (black).
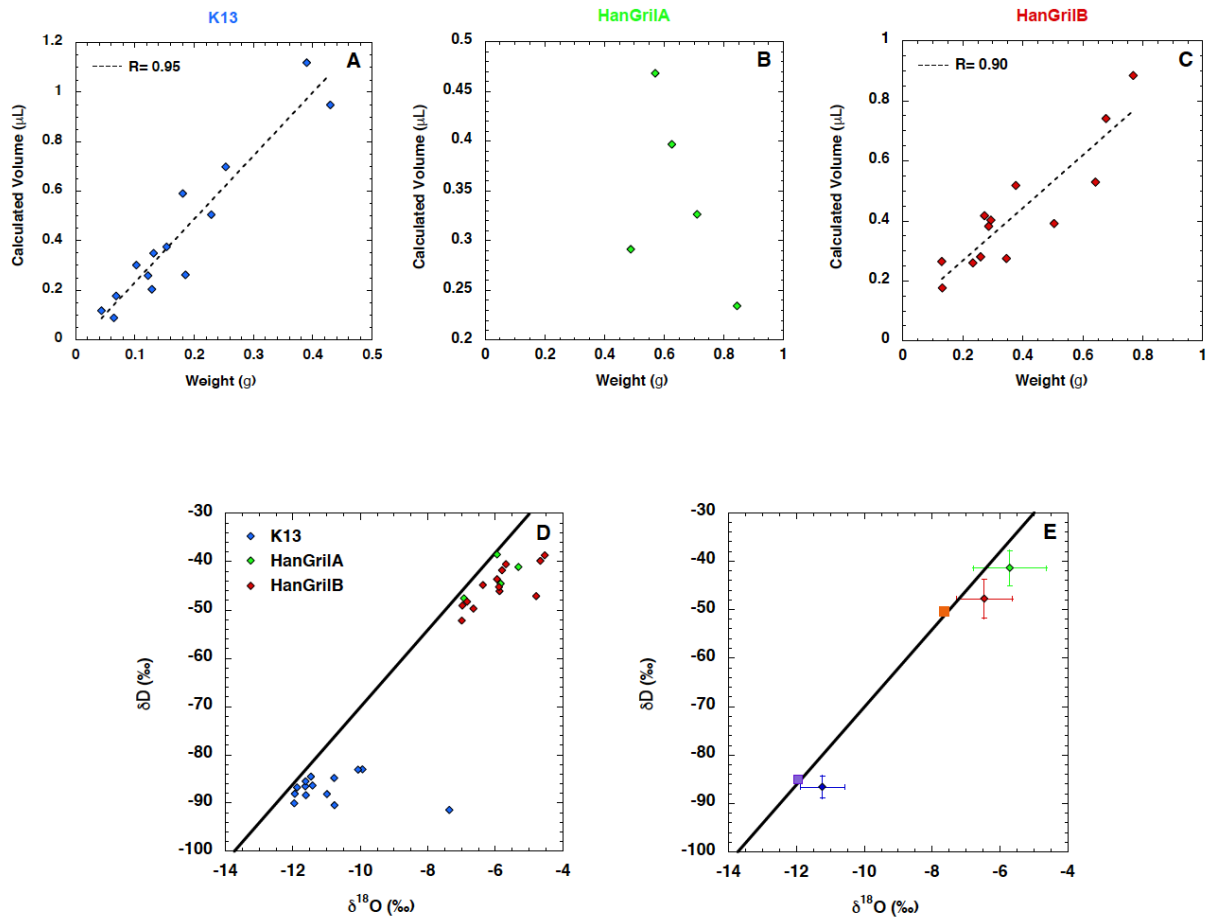
Figure 8: Top panel: relationship between quantity of calcite (in g) and quantity of water released (in µL) for the three speleothem samples: K13, HanGrilA, and HanGrilB. Plot D: Relationship between fluid inclusions $\delta^{18}O$ and δD of all three speleothem samples. Plot E: The mean fluid inclusion $\delta^{18}O$ and δD of all the speleothem samples, except the one outlined on plot D. are potted with their associated error represented by 1σ. The black line on plot D. and E. corresponds to the Global Meteoric Water Line (GMWL) (Craig, 1961).
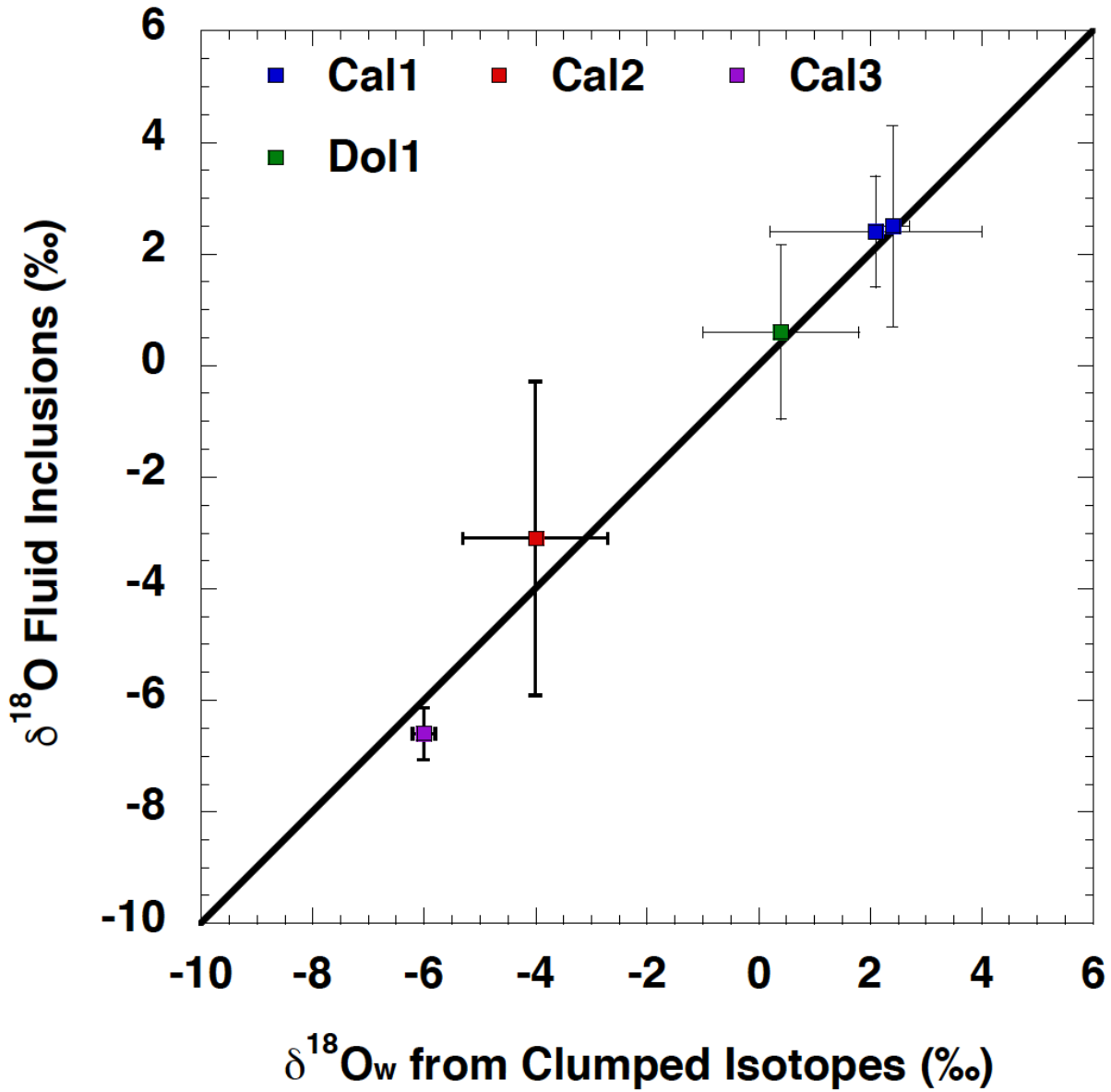
Figure 9: Cross-plot between fluid inclusions $\delta^{18}O$ values measured with the analytical line presented in this paper and $\delta^{18}O_w$ composition independently calculated from Δ_{47} analyses on the host carbonate. The two methods were applied on the same cement specimens. The black line represents the 1:1 relationship. Error bars on the x axis correspond to the associated error of the Δ_{47} analyses and error bars on the y axis correspond to one standard deviation of the mean of the fluid inclusion values.

Certified Standards		
	$\delta^{18}O$ (1σ)	δD (1σ)
- 5 ‰	-5.1 ± 0.2	-31 ± 1
- 8 ‰	-8.1 ± 0.2	-56 ± 1
- 10 ‰	-10.0 ± 0.2	-70 ± 1
- 30 ‰	-30.1 ± 0.2	-232 ± 1
ESKA	-13.96 ± 0.05	-100.15 ± 1.12
MAZA	-1.18 ± 0.05	1.28 ± 0.91
NAN	-9.46 ± 0.04	-66.05 ± 0.69
DOME C	-52.66 ± 0.07	-412.80 ± 0.91

Table 1: $\delta^{18}O$ and δD values of certified water standards and their respective 1σ error. Each values were all calibrated against internationals standards: the Vienna Standard Mean Ocean Water (VSMOW), the Greenland Ice Sheet Precipitation (GISP), and the Standard Light Antarctic Precipitation (SLAP) on a mass spectrometer (IRMS Thermo Finnigan Delta Plus, equipped with an equilibrating bench).

	H$_2$0	STDEV	Std Error	δ^{18}O	STDEV	Std Error	δD	STDEV	Std Error
January									
19/01/2015	**8452.36**	14.26	0.45	-6.18	0.21	0.01	-48.90	3.64	0.11
	9419.24	10.33	0.33	-6.20	0.20	0.01	-48.72	3.31	0.10
	10335.48	18.13	0.57	-6.24	0.20	0.01	-48.53	2.98	0.09
	11255.13	44.62	1.41	-6.23	0.21	0.01	-48.32	2.70	0.09
	12158.17	84.65	2.68	-6.27	0.20	0.01	-48.16	2.53	0.08
	13109.99	24.71	0.78	-6.23	0.20	0.01	-48.14	2.29	0.07
20/01/2015a	**3619.77**	11.93	0.38	-6.10	0.32	0.01	-49.26	8.74	0.28
	4560.79	23.34	0.74	-6.12	0.27	0.01	-48.51	7.08	0.22
	5485.09	12.18	0.39	-6.08	0.25	0.01	-48.55	5.63	0.18
	6402.45	6.87	0.22	-6.07	0.23	0.01	-48.17	4.93	0.16
	7299.74	13.00	0.41	-6.16	0.22	0.01	-47.81	4.26	0.13
	8255.17	13.76	0.44	-6.11	0.22	0.01	-47.90	3.68	0.12
20/01/2015b	**12647.61**	30.28	0.96	-6.06	0.20	0.01	-47.40	2.37	0.08
	13600.38	92.95	2.94	-6.06	0.21	0.01	-47.43	2.17	0.07
	14436.91	49.87	1.58	-5.98	0.19	0.01	-47.44	2.05	0.06
27/01/2015	**7208.42**	10.22	0.32	-15.55	0.23	0.01	-127.68	4.35	0.14
	8226.43	12.42	0.39	-15.64	0.21	0.01	-127.65	3.79	0.12
	8719.51	41.98	1.33	-15.62	0.20	0.01	-127.55	3.56	0.11
	9700.07	5.74	0.18	-15.64	0.21	0.01	-127.40	3.11	0.10
	10700.98	11.16	0.35	-15.59	0.20	0.01	-127.45	2.75	0.09
	11762.87	10.31	0.33	-15.56	0.21	0.01	-127.12	2.53	0.08
	12744.00	13.39	0.42	-15.57	0.19	0.01	-126.92	2.28	0.07
	13768.24	7.85	0.25	-15.57	0.20	0.01	-126.78	2.12	0.07
	14828.56	20.46	0.65	-15.59	0.20	0.01	-126.61	1.87	0.06
	15947.84	27.03	0.85	-15.66	0.20	0.01	-126.41	1.81	0.06
	17130.15	28.12	0.89	-15.46	0.20	0.01	-126.50	1.75	0.06
	21017.82	103.38	3.27	-15.43	0.21	0.01	-125.54	1.42	0.04
	20105.13	46.29	1.46	-15.44	0.21	0.01	-125.57	1.44	0.05
September									
08/09/2015	**10397.76**	7.98	0.25	-7.93	0.20	0.01	-50.72	2.72	0.09
	8481.75	10.27	0.32	-7.98	0.21	0.01	-50.82	3.16	0.10
	7478.16	9.28	0.29	-8.06	0.22	0.01	-50.78	3.89	0.12
	6682.66	11.55	0.37	-8.03	0.23	0.01	-50.92	4.29	0.14

	6133.62	12.96	0.41	-8.06	0.23	0.01	-50.56	4.82	0.15
	5668.19	14.66	0.46	-8.02	0.23	0.01	-50.99	5.09	0.16
	5217.27	16.19	0.51	-8.09	0.26	0.01	-51.27	5.62	0.18
09/09/2015	16779	13.90	0.44	-7.84	0.20	0.01	-49.91	1.59	0.05
	11242	13.49	0.43	-7.98	0.18	0.01	-50.27	2.50	0.08
	10528	12.58	0.40	-8.00	0.20	0.01	-50.35	2.68	0.08
	6529	12.81	0.41	-7.87	0.22	0.01	-50.66	4.49	0.14
	4919	15.55	0.49	-7.73	0.25	0.01	-51.07	5.83	0.18
15/09/2015	2161	9.27	0.29	-9.40	0.44	0.01	-58.69	13.24	0.42
	2375	14.58	0.46	-9.27	0.42	0.01	-58.47	12.78	0.40
	3389	12.80	0.40	-9.13	0.32	0.01	-57.55	8.98	0.28
	3958	10.60	0.34	-9.20	0.29	0.01	-57.41	7.59	0.24
	4982	8.29	0.26	-9.08	0.24	0.01	-57.17	5.84	0.18
	5970	7.32	0.23	-9.07	0.23	0.01	-56.70	5.01	0.16
	6582	6.78	0.21	-9.12	0.23	0.01	-56.72	4.43	0.14
	7160	7.46	0.24	-9.06	0.21	0.01	-56.71	3.98	0.13
	7799	5.71	0.18	-9.04	0.22	0.01	-56.80	3.66	0.12
	8380	4.80	0.15	-9.05	0.21	0.01	-56.50	3.52	0.11
	9018	6.04	0.19	-9.02	0.21	0.01	-56.43	3.19	0.10
	9599	7.15	0.23	-9.00	0.21	0.01	-56.27	3.11	0.10
	10205	6.83	0.22	-9.02	0.20	0.01	-56.38	2.78	0.09
26/09/2015	8320	5.64	0.18	-7.98	0.21	0.01	-51.01	3.29	0.10
	9199	16.51	0.52	-7.94	0.21	0.01	-50.89	3.08	0.10
	10346	13.24	0.42	-7.93	0.21	0.01	-50.52	2.63	0.08
	12367	14.08	0.45	-7.84	0.21	0.01	-50.30	2.22	0.07
	14373	20.78	0.66	-7.89	0.19	0.01	-49.90	1.87	0.06
	15748	44.50	1.41	-7.88	0.21	0.01	-49.80	1.70	0.05
	17526	31.52	1.00	-7.85	0.20	0.01	-49.73	1.52	0.05
29/09/2015	15041	19.46	0.62	-10.97	0.21	0.01	-72.38	1.81	0.06
	15763	9.54	0.30	-10.86	0.20	0.01	-72.39	1.71	0.05
30/09/2015	19422	24.31	0.77	-10.82	0.21	0.01	-71.77	1.46	0.05
	19316	20.11	0.64	-10.91	0.21	0.01	-71.67	1.40	0.04
	17226	17.31	0.55	-10.90	0.21	0.01	-71.80	1.58	0.05
	19019	17.33	0.55	-10.87	0.20	0.01	-71.79	1.42	0.05
	17961	12.24	0.39	-10.80	0.20	0.01	-71.89	1.53	0.05

	18372	21.41	0.68	-10.88	0.21	0.01	-71.80	1.44	0.05
October								
01/10/2015	**19548**	33.33	1.05	-10.68	0.21	0.01	-71.29	1.40	0.04
	20479	19.15	0.61	-10.62	0.21	0.01	-71.12	1.34	0.04
	21473	19.61	0.62	-10.53	0.21	0.01	-71.06	1.29	0.04
	22335	24.83	0.79	-10.57	0.20	0.01	-71.08	1.21	0.04
	23365	40.23	1.27	-10.58	0.21	0.01	-70.92	1.15	0.04

Table 2: Summary of the data used to determine the water background stability on Figure 3. The various set backgrounds were analyzed over a period of three hours and we averaged the data over the last 30 minutes. For each set backgrounds, the mean water concentration (H_2O), $\delta^{18}O$ and δD, are indicated along with their standard deviation (STDEV) and standard error (Std Error).

	Date	Certified Standards			
		- 5 ‰	- 8 ‰	ESKA	MAZA
Calibration	12/13/2015	4	4	4	4
	12/15/2015	4	3	4	4
	12/16/2015	2	4	6	6
	12/17/2015	3	3	3	3
	12/18/2015	4	3	3	5
	Total	**17**	**17**	**20**	**22**

		- 10 ‰		NAN		DOME C		- 30 ‰	
	Date	0.3µL	0.5µL	0.3µL	0.5µL	0.3µL	0.5µL	0.3µL	0.5µL
Extra values	10/12/2015		4		4				
	10/15/2015		5						
	11/03/2015	2				3			
	11/04/2015	3				3			
	11/05/2015	4				4			
	11/27/2015	3				5		3	
	12/08/2015	3				2		3	
	12/09/2015	2				3		1	
	12/10/2015	6							
	Total	**32**		**4**		**20**		**7**	

Table 3: Summary of the data used to determine calibration equations on Figure 5. Top panel are the number of injections of 0.5 μL of certified standards that we used to establish calibration equations. Bottom panel are the number of injections per day of other certified standards that were used to verify the linearity of the calibration presented in Figure 5.

	Calibration equations for $\delta^{18}O$			Calibration equations for δD		
	Slope	Intercept	R^2	Slope	Intercept	R^2
12/13/2015	0.968 ± 0.008	1.282 ± 0.079	0.999	0.969 ± 0.009	-2.165 ± 0.545	0.999
12/15/2015	0.972 ± 0.008	1.376 ± 0.088	0.999	0.965 ± 0.010	-1.574 ± 0.648	0.998
12/16/2015	0.984 ± 0.012	1.443 ± 1.130	0.997	0.967 ± 0.009	-1.833 ± 0.597	0.999
12/17/2015	1.001 ± 0.012	1.566 ± 0.118	0.998	0.955 ± 0.004	-1.596 ± 0.262	0.999
12/18/2015	0.983 ± 0.012	1.284 ± 0.108	0.998	0.976 ± 0.012	-1.191 ± 0.640	0.998
Mean	**0.979 ± 0.005**	**1.371 ± 0.049**	**0.999**	**0.967 ± 0.004**	**-1.675 ± 0.261**	**0.999**

Table 4: Regression coefficients, slopes, intercepts, and associated error from linear regressions presented in Figure 5.A. All the values are significant at 99%.

	Speleothem samples					Diagenetic samples			
	Size (g)	Water (μL)	δ^{18}O	δD		Size (g)	Water (μL)	δ^{18}O	δD
K13					**BUF 4**				
	0.43	0.95	-10.78	-84.78		0.79	0.18	-6.14	-29.65
	0.13	0.20	-10.99	-88.12		0.99	0.48	-6.55	-31.45
	0.19	0.26	-11.61	-88.39		0.88	0.32	-7.08	-32.47
	0.39	1.12	-11.63	-86.54	**BEB J8**				
	0.13	0.35	-11.87	-86.75		0.77	0.34	2.17	-22.96
	0.23	0.51	-11.47	-84.54		0.59	0.3	1.60	-19.70
	0.15	0.37	-11.94	-88.08		0.92	0.52	2.14	-21.81
	0.12	0.26	-11.96	-90.02		0.88	0.27	4.07	-10.99
	0.07	0.18	-9.94	-83.05	**RN21**				
	0.18	0.59	-11.62	-85.51		0.78	0.03	-1.10	-38.64
	0.25	0.70	-11.42	-86.35		1.03	0.01	-5.08	-49.83
	0.04	0.12	-10.77	-90.46	**VPU4**				
	0.06	0.09	-7.37	-91.40		0.6	0.15	1.65	-15.98
	0.10	0.30	-10.07	-83.09		0.97	0.19	-0.55	-18.73
HanGrilA					**VPU9**				
	0.49	0.29	-3.63	-38.13		0.66	0.27	4.07	-13.92
	0.63	0.40	-5.85	-44.54		0.96	0.52	1.64	-19.89
	0.71	0.33	-5.32	-41.09		0.93	0.44	1.95	-19.80
	0.57	0.47	-5.95	-38.47		1.03	0.52	1.83	-20.72
	0.84	0.23	-6.93	-47.55					
HanGrilB									
	0.50	0.39	-7.00	-52.19					
	0.64	0.53	-6.65	-49.70					
	0.77	0.88	-6.98	-49.04					
	0.38	0.52	-5.88	-46.09					
	0.29	0.40	-5.89	-45.25					
	0.68	0.74	-6.84	-48.29					
	0.29	0.38	-5.95	-43.62					
	0.13	0.26	-5.80	-41.75					
	0.13	0.18	-4.67	-39.84					
	0.34	0.28	-4.54	-38.65					
	0.27	0.42	-4.79	-47.14					
	0.26	0.28	-6.37	-44.81					
	0.23	0.26	-5.69	-40.49					

Table 5: Summary of both speleothems (left side of the table) and diagenetic carbonates (right side of the table) crushes. Weight of the calcite sample (in g) and water released during the crushing determined using linear regression presented Figure 5.

Name	δ¹⁸Owater ‰	δDwater ‰	n
K13	-11.24 ± 0.65	-86.59 ± 2.29	13
HanGrilA	-5.54 ± 1.08	-41.96 ± 3.62	5
HanGrilB	-5.93 ± 0.82	-45.14 ± 3.98	13

> 0.3 mL

Name	δ¹⁸Owater ‰	δDwater ‰	n
K13	-11.53 ± 0.36	-86.08 ± 1.14	7
HanGrilA	-5.71 ± 0.28	-41.36 ± 2.49	3
HanGrilB	-6.14 ± 0.70	-47.02 ± 2.02	7

Table 6: Speleothem sample average δ^{18}O and δD values. Uncertainties are reported as one standard deviation of the mean. (n) is the number of replicate measurements used to create the mean value. Top table: all the speleothem samples used in this study and presented in Fig. 7a.b.c expect the one out of range in Fig. 7d. Bottom table: speleothem samples for which the quantity of water released is superior to 0.3μL.

Korallgrottan Cave

δ18O	δD	n
-11.95 ± 0.13	-85.03 ± 0.77	9

Han-sur-Lesse Cave

δ18O	δD	n
-7.65 ± 0.04	-50.34 ± 0.39	36

Table 7: Isotopic composition of Korallgrottan and Han-sur-Lesse cave drip water. Uncertainties are reported as one standard deviation of the mean of all (n) samples.

			CLUMPED ISOTOPE RESULTS					CRUSH LEACH RESULTS		
Name	Mineralogy	Phase	Δ_{47} ‰	$\delta^{18}O_c$ ‰	n	$T(\Delta_{47})$ °C	$\delta^{18}O_{water}$ ‰	$\delta^{18}O$ ‰	δD ‰	n
BEBJ8	calcite	Cal1	0.586 ± 0.004	-7.23 ± 0.03	3	66 ± 4	2.4 ± 0.3	2.5 ± 1.1	-18.9 ± 5.4	4
VPU9	calcite	Cal1	0.600 ± 0.025	-7.21 ± 0.03	3	64 ± 11	2.1 ± 1.9	2.4 ± 1.1	-18.6 ± 3.1	4
VPU4	dolomite	Dol1	0.537 ± 0.016	-9.39 ± 0.04	3	91 ± 10	0.4 ± 1.4	0.6 ± 1.6	-17.4 ± 1.9	2
RN21	calcite	Cal2	0.559 ± 0.015	-15.26 ± 0.01	3	79 ± 8	-4.0 ± 1.3	-3.1 ± 2.8	-44.2 ± 7.9	2
BUF4	calcite	Cal3	0.642 ± 0.021	-11.78 ± 0.83	3	42 ± 11	-6.0 ± 0.2	-6.6 ± 0.5	-31.2 ± 1.4	3

Table 8: Summary of stable isotope results from diagenetic samples. On the left is reported the stable isotope data acquired on the host mineral and on the right, is reported the data directly measured on micro-volumes of fluid inclusions water. (n) is the number of replicate measurements. Δ_{47} values are from Mangenot et al. (2018). Uncertainties are reported as one standard deviation of the mean. $T(\Delta_{47})$ values are paleotemperatures calculated using the inter-laboratory composite Δ_{47}-T calibration of Bonifacie et al., 2017. $\delta^{18}O_c$ is the oxygen isotope composition of the carbonate. $\delta^{18}O_{water}$ is the mineralizing waters isotopic composition back-calculated using $T\Delta_{47}$, $\delta^{18}O_c$, and the equations of fractionation of oxygen isotopes between the carbonate and water of either O'Neil et al. (1969) for calcite and Horita (2014) for dolomite. Reported uncertainties in $\delta^{18}O_{water}$ values are only related to uncertainties associated to Δ_{47} temperatures estimations. Crush Leach $\delta^{18}O$ and δD are the isotopic composition of the fluid inclusions measured using the line presented in this study.